MODELLING THE ALUMINIUM SMELTING CELL MASS AND ENERGY BALANCE – A TOOL BASED ON THE 1ST LAW OF THERMODYNAMICS

Vanderlei Gusberti[(1)], Dagoberto S. Severo[(1)], Barry J. Welch[(2)], Maria Skyllas-Kazacos[(2)].

1) CAETE Engenharia, Rua Caeté 162, Porto Alegre RS– Brazil

caete@caetebr.com

2) School of Chemical Engineering, University of New South Wales, Sydney, NSW, 2052, Australia

Abstract

The understanding and prediction of the electrolysis cell heat balance is a key factor for efficient cell operation and extended cell life. In the past, many cell heat balance models have been developed in order to calculate the cell operation window. These models relied on curve fitted data obtained decades ago and also disregarded many cell mass inputs and outputs.

The thermal balance model presented in this work is entirely based on the first law of thermodynamics. This is a more robust and general approach, valid for any type of cell, any size, steady state or transient calculations. Unlike the traditional models, the extended cell control volume suggested by Welch and Keniry (2000) [1] is adopted. This allows to include the under hood reactions, such as anode carbon, CO and COS oxidations. The influence of the cell duct flow rate on the heat losses can also be studied.

A user-friendly software tool for predicting the cell energy balance was developed. For a given cell design, the user can modify cell operation parameters quickly obtaining the new resulting situation. The new modelling tool is applied to an operating cell and the results are compared with "classical" methodology.

Keywords: aluminium cell modelling, mass balance, energy balance.

Introduction

The behaviour of modern cells is the result of a wide range of parameters. Some parameters are defined by the cell design (cell thermal insulation, maximum electrical current capacity, magnetohydrodynamic condition), while other parameters are controlled automatically by a computerized system (cell voltage drop, alumina feeding) and there are also parameters dependent on human interaction (anode changing, anode covering, bath corrections, aluminium tapping). Optimum values have to be pursued by plant operation. In the large scale production, any small process improvement can lead to relevant energy saving.

Nowadays, thermal equilibrium of aluminium reduction cells is becoming more and more constrained with the increase of the cell size, squeezing of ACD and energy saving needs. Therefore, fine tuning of cell heat balance is very important and requires more accurate cell mass and energy balance understanding, control and prediction.

In the past, many heat balance models considered only carbon, alumina, aluminium, CO and CO_2 in the material balance. In the voltage equations published in [2], even the excess of carbon consumption is neglected. Nevertheless this approach is popular among analysts [3, 4], probably due to its simplicity.

Haupin´s [2] assumptions for CO/CO_2 output rates were proposed in the 1950s [5], when it was believed that the only source of current efficiency loss was the reoxidation reaction. At that time, anode dressing was different, usually using pure alumina instead of mixing recycled bath. Nowadays, ACD is squeezed as much as possible causing important current efficiency losses through anode spikes. This fact changes the prediction of CO/CO_2 formation inside the cell, as well as the resulting energy balance.

This paper presents the following features implemented in a new cell energy balance modelling approach:

- Extension of the cell control volume to include the cell hooding as suggested by Welch and Keniry [1]. All previous models do not include the cell under hood space in the control volume, but important exothermic reactions occur at that place, influencing heat balance.

- Better cell mass balance representing a more complete set of materials flow. This is an important step to achieve more accurate cell energy balance entirely based on the 1st law of thermodynamics, independent of the curve fitted data of the voltage equations. This includes unused carbon and anode changing materials flow, bath corrections and heat losses associated with the cavity cleaning procedure.

- The convective heat transfer between ledge and the cell internal liquids is a source of uncertainty in the cell heat balance. In recent years, bath flow is being more studied in physical scale models [6] and numerical models [7]. In this work, 3D fluid flow modelling developed at CAETE will be used [7] in order to account for the MHD flow and the bubble-induced flow inside the bath.

- An auxiliary CFD model dedicated to predicting the cell gas duct temperature was developed. Results are dependent on cell thermal state, average cover thickness and gas duct flow rate.

Mathematical modelling of a complete cell mass and energy flow provides a tool for forecasting the cell response to state perturbations and for optimising the necessary actions to bring the cell state inside the desired targets. It can also be used for predictions of bath correction and fluoride evolution levels. Operating the cell in an optimal state envelope saves energy and raw materials and, as well, decreases the harmful emission levels to the environment.

The main objective of this research is to provide a tool for engineers to study cell operation parameters, quickly performing many virtual tests, with immediate response. The program can help process engineers to find the cell's optimum operation window (combination of bath chemistry, ACD, bath superheat, voltage drop, cell current), increasing the process efficiency. It is necessary to build up a modelling system capable of using all the power of 3D sub-models in order to supply detailed information to a global cell energy balance model. The global balance model can then quickly re-run many operational setups in order to obtain and plot an operational window chart for a given cell technology. The Figure 1 shows a generic

representation of the cell's operating window. The thermal limits are found approximately at constant energy input lines (red). The ACD limit (blue line) is the lowest interpolar distance where current efficiency can be maintained at appropriate levels, governed by a complex combination of factors such as: CO_2 bubbles flow, MHD instability and bath volume to dissolve alumina.

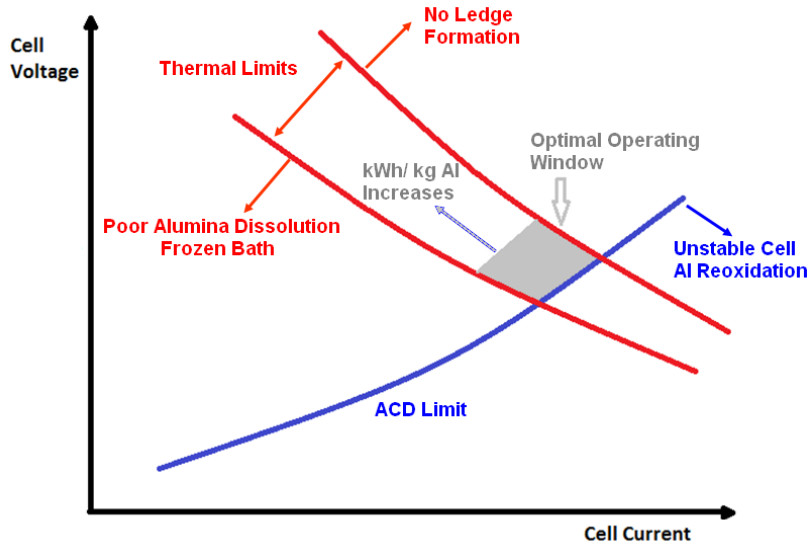

Figure 1: Voltage operational window diagram

Cell Mass Balance

The basis for the proposed aluminium reduction process model is the first law of thermodynamics. Consequently, mass balance for a given control volume must be established on an elemental basis. In general, the mass conservation law is applied in the steady state form for each species.

$$\dot{w}_{in\_i} + \dot{w}_{generated} - \dot{w}_{out\_i} - \dot{w}_{consumed} = 0 \qquad (1)$$

Where $\dot{w}$ is the massflow rate in [kg/day] of a substance "i". Many material flows are usually monitored by the smelters, for example: aluminium, alumina, carbon, AlF_3, alumina impurities, fluorides. However some mass flow inputs or outputs must be obtained by additional measurements or analytical techniques, such as gaseous emissions: H_2O, SO_2, CO_2, etc.

Control Volume Definition: New Approach

The choice of the control volume boundaries is determinant for a successful mass and energy balance model. In general, earlier models [4, 8, 9, 10, 11, 12, 13] usually worked with a control volume involving the cell interior and cover as shown in Figure 2. This approach was useful to study chemical-physical processes occurring only inside the bath layer, disregarding many reactions that take place under the cell hood, but above the cell crust. These reactions are responsible for an important amount of cell heat source, since most of them are combustion reactions.

A more extended control volume was proposed by Welch and Keniry [1] as a future option for improving aluminium cells thermal modelling. To the best of the authors' knowledge, it was not implemented up to now. It comprises the entire hooded cell, allowing the cell gases to cross the control volume at the cell hood gaps and gas collection duct entrance. The advantage of this extended cell control volume is the elimination of many uncertainties of the proportions and contributions of various intermediary reactions occurring under the cell hooding.

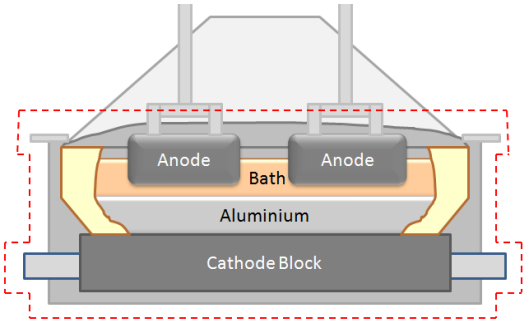

Figure 2: Control volume adopted by earlier heat balance models

In the present work, this new approach for control volume is implemented as the basis for the cell mass and energy balance. The main difficulty is that it implies the knowledge of cell duct flow rate, temperature and composition. However many species' flow rates can be deduced by analytical methods and the duct temperature and flow rate are easy to measure and are even monitored regularly by some smelters. Additionally, CFD auxiliary models can be implemented in order to determine duct flow rate and temperature. The Figure 3 presents the aluminium cell control volume, including all relevant species' flows considered in the present modelling approach.

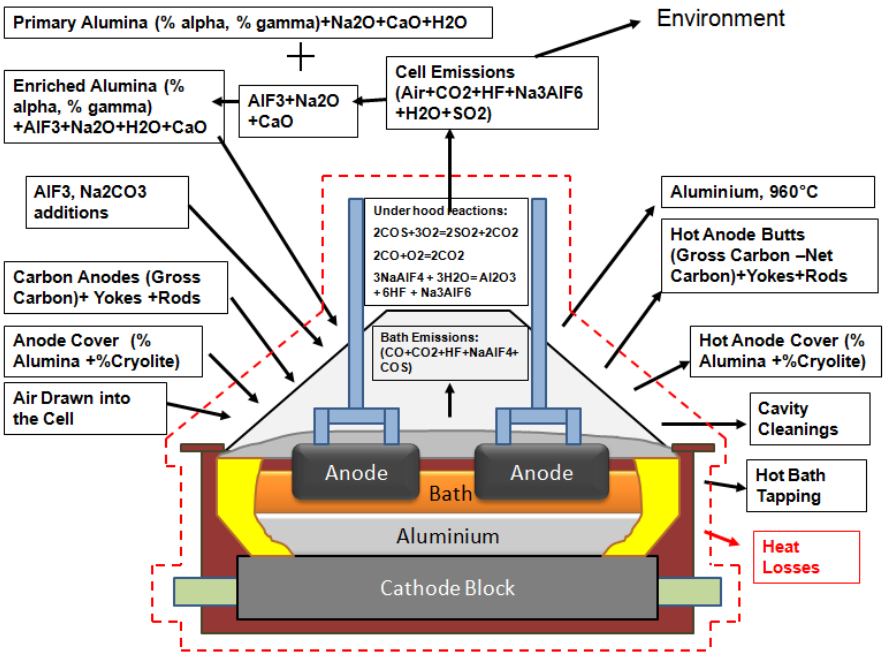

Figure 3: Relevant materials flow through the cell control volume

The best option to represent the massflow quantities is in units of kg of species per ton of produced metallic aluminium [kg /ton Al], since the aluminium production rate is very well measured. It also enables the comparison of performance between different cell technologies and size.

Material Inputs

Material inputs comprise all mass crossing the control volume from the outside to the cell interior. The major species are alumina and carbon (anodes), necessary for the alumina reduction reaction. However, for a sufficiently good mass and energy balance, considering only these species is too simplistic.

Alumina Feeding, Dry Scrubbing and Alumina Impurities

The pure Al_2O_3 required to make aluminium can easily be calculated by stoichiometry, resulting in 1889 kg/ton Al. However, alumina provided to the cell is in fact ~98% Al_2O_3, the rest being composed of impurities. Another important aspect associated with alumina is the phase content of alumina fed into the cell. Nowadays, it is common to use aluminas rich in gamma phase (more than 90%) and low alpha phase content (less than 10%). Different alumina phases present different enthalpy and thus influence the energy balance of the cell.

In the smelters, dry scrubbing is applied to the cell exhaust gases in order to collect the cell emissions harmful to the environment. "Primary" alumina (also called "fresh" alumina) is injected into the cell exhaust gases stream. Some impurities are already present in primary alumina (Na_2O, CaO, H_2O). This mix travels to the bag houses where the clean gases are separated from the, now called, "secondary" alumina (or "enriched" alumina, or "reacted" alumina). The secondary alumina is then directed to the aluminium reduction cell feeders, recycling almost all cell emissions (typically, more than 99.9%). The Figure 4 shows, schematically, the alumina and gases streams allowing the recycling of cell emissions.

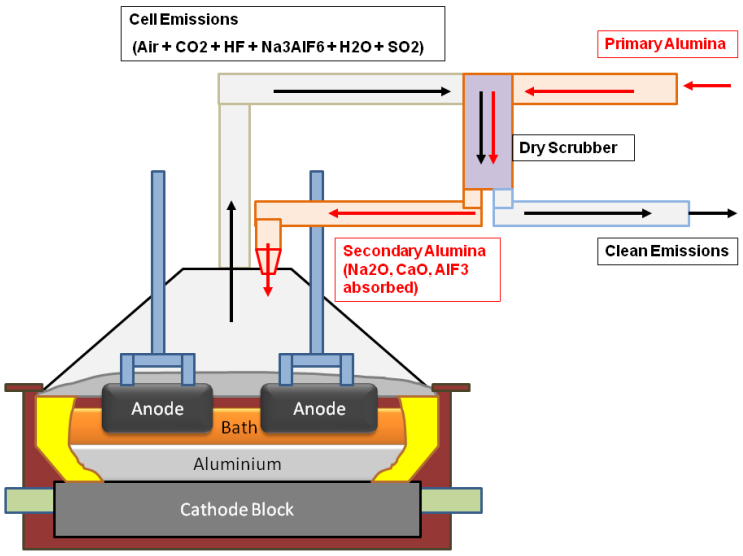

Figure 4: Alumina and cell duct gases streams in dry scrubbing process

The most important species of interest for this process are the recycled fluorides (mainly HF and $NaAlF_4$), but other impurities also are recycled, such as Fe. For the mass and energy balance purposes, the relevant impurities to be considered in this work are those influencing the bath chemistry (Na_2O, CaO, AlF_3), H_2O and adsorbed OH^- that is correlated to the L.O.I. They need to be measured in primary and secondary alumina. The total alumina demand of the reduction cell is typically around 1940 kg/ton Al, including impurities. Not all alumina demand is provided by the alumina feeders. Eventually part of the added cover falls into the bath, providing up to 10% of alumina consumed. All the secondary alumina impurities must be heated to reach the bath temperature.

Bath Corrections: AlF_3 and Na_2CO_3 Additions

One of the key factors in order to obtain optimal aluminium production efficiency is to maintain the bath composition as stable as possible around specified target values. Usually, the maintenance of the %AlF_3 between 10-13% is desired because it lowers the melting point of bath to ~950°C, improving current efficiency. There are two basic oxides entering the cell together with alumina: Na_2O and CaO. In the bath, they will form cryolite and CaF_2, according to equations (2) and (3) , and consuming AlF_3 continuously.

$$3Na_2O + 4AlF_3 \rightarrow 2Na_3AlF_6 + Al_2O_3 \quad (2)$$

$$3CaO + 2AlF_3 \rightarrow 3CaF_2 + Al_2O_3 \quad (3)$$

Aluminium fluoride must be regularly added into the cell to readjust bath chemistry back to the targets. The AlF_3 addition rate is well predictable [14], according to alumina composition and scrubber efficiency. The deficit in AlF_3 is originated by the primary alumina composition, since the AlF_3 and Na_2O gained in the scrubbers are produced by the bath and come back in a closed loop.

Another factor influencing the AlF_3 demand is the sodium uptake by the cathodes. Depending on the cathode type, AlF_3 demand is below the presented prediction because part of the sodium provided to the cell by the alumina is absorbed into the cathode in the early months of cathode life. Occasionally, the bath AlF_3 concentration is found to be higher than the target, caused by a number of reasons:

- Excess of addition by wrong AlF_3 demand prediction;
- Change in AlF_3 concentration target;
- Sodium uptake higher than expected by cathodes;

In this case, sodium carbonate (Na_2CO_3) is added in order to neutralize the aluminium fluoride, see equation (4). Sodium carbonate additions occur much less often than aluminium fluoride additions.

$$4AlF_3 + 3Na_2CO_3 \rightarrow 2Na_3AlF_6 + Al_2O_3 + 3CO_2 \quad (4)$$

Carbon and Anode Assembly Material Inputs

Electrolytic oxidation of the carbon anode reduces the energy requirement of the Hall-Heroult process compared to an inert anode and makes the aluminium reduction feasible and efficient at temperatures around 960°C. Carbon anodes enter the control volume accompanied by

anode stubs, yokes and guide rods. These materials do not react inside the control volume, but they consume energy to be heated up. Anodes are gradually consumed at a predictable rate, and replaced when necessary. In prebake technologies, not all carbon is consumed and ~20% of original carbon is retrieved from the cell in the form of hot anode butt (at ~800°C). The theoretical minimum carbon requirement, calculated by stoichiometry, is 333.4 kg/ton Al. In real cell operation, however, a number of factors are responsible for increasing this consumption rate up to ~550 kg/ton Al considering the total carbon provided to the cell (gross carbon):

- Part of carbon is not used (anode butt) and is recycled. This makes the net carbon consumption in the range of 400-450 kg/ton Al;
- Part of carbon is consumed by Boudouard reaction;
- Part of carbon is lost by oxidation when hot carbon is in contact with air;
- Part of carbon is lost in the form of carbon dust.
- Part of anode mass is formed by impurities, typically Sulphur 1.5-3%. It forms two gases during the anode consumption, COS and SO_2, influencing cell emissions composition;

The amount of carbon wasted by the above processes is dependent on cell working practices and anode quality. As a consequence, a reliable prediction is very difficult, although aluminium smelters usually keep track of gross and net carbon consumption.

Anode Cover Addition

During the anode change procedure, there is addition of dressing cover over the anodes. The careful covering of the anodes is a key aspect for successful cell operation. In modern cells, the cover is a mix of crushed bath and alumina, the proportions being determined by smelter operations. A certain amount of cover has to be replaced at each anode change because:

- Part of the cover is carried out of the cell with the anode butt;
- Part of the old cover falls into the bath during the break of the consolidated crust;
- Part of the cover is spilt into the bath during the dressing of new anodes;

With the cover, a certain amount of alumina falls into the bath reducing the alumina demand from the alumina feeders (up to 10%). For the same reason, bath level tends to increase because crushed bath is melted when part of the cover falls into the cavity. Sometimes fallen cover does not dissolve and generates the so called “bottom sludge” or “muck” on the cathode surface. Cathode cleaning procedure will be discussed in the materials output subsection. All these contributions must be estimated for the cell materials balance.

Potroom Air Drawn into the Cell

More than 95% of the gases collected by the cell exhaust system are originally potroom air drawn into the cell by the negative pressure present under the cell hood. The remaining ~5% is produced inside the cell, mainly in the bath. The potroom air provides also oxygen and water for some chemical reactions. With the information of exhaust flow mix and the knowledge of cell internal processes, it is possible to quantify the amount of air sucked into the cell. In this work the composition of air entering in the cell is considered as atmospheric

standard composed of the species: N_2, O_2, CO_2, Ar, H_2O. Other minor inert gas contributions present in atmospheric air are not considered relevant for the mass and energy balance.

Material Outputs

Material output is considered as any amount of mass crossing the control volume from the inside to the outside.

Aluminium Tapping

Aluminium metal is produced by electrolysis and its rate is governed by Faraday' law at a certain current efficiency. Typically the metal is tapped out once a day and it leaves the control volume at ~960°C.

Spent Anode Assembly Removal

Due to practical reasons, a fraction of the carbon anode (anode "butt") must leave the cell attached to the rest of the anode assembly to protect the steel parts from the bath attack. Part of the sulphur content associated with the new anode also leaves the cell untouched inside the anode butt. Other assembly parts leave the cell (yoke, cast iron collars, guide rod) at high temperatures as shown in Figure 5. In addition, part of anode cover is also removed with the butt.

Cathode Surface Cleaning

Modern cell operation practices recommend cleaning of the cell cavity during the anode change procedure (Figure 6). If the cathode block's surface is not in good contact with the metal, the electrical current path is disturbed, as well the entire cell behaviour in many aspects (electrical, thermal, magnetics, fluid flow). Cavity cleaning material can be of different origins and nature:

- "Sludge" or "muck" is formed by undissolved alumina that settles below the metal layer. This alumina can be of feeder origin or part of cover material fallen into the bath.
- During the anode removal procedure, part of consolidate cover (crust) is broken in solid pieces and they are very likely to deposit over the cathode blocks.
- Pieces of broken carbon anode.

Figure 5: Spent anode butt being retrieved from the cell, source: Iffert Thesis (2007) [15]

Figure 6: Cathode cleaning material being removed from cell

In the mass and energy balance, it is observed that the cleaning device crosses the control volume boundary, entering the cell in a cold state and leaving at higher temperature, thus removing a certain amount of energy from the cell, associated with the enthalpy difference of the equipment. Sometimes the heat stored in the cleaning device is in the order of 0.1 [kg/ton Al] and it should be taken into account in order to achieve precise heat balance calculations.

Bath Tapping

There are two sources of bath formation in the cell:

a) The neutralization of Na_2O and CaO entering the cell control volume by AlF_3. Formation of Na_3AlF_6 and CaF_2 occurs according to equations (2) and (3).

b) Cover spillage into the bath. The alumina part of the cover spillage may be consumed to make aluminium metal. However, the crushed bath will likely melt and increase the bath volume.

The rate of bath production by mechanism a) is very well predictable by knowing the alumina impurities composition. The amount formed by process b) is more complex to analyse and is dependent on cell working practices and strategies.

Cell Emissions

The cell duct emissions are composed, in a general manner, of the air drawn into the cell, including humidity, plus the gases generated inside the control volume minus the gases consumed by the cell inside the control volume. There are many transformations inside the aluminium cell involving gases as reactants and/or products. The chemical reactions involving gaseous species that are considered in this work as of importance for the heat and mass balance are listed below:

- Alumina reduction to produce metal:

$$2Al_2O_3 + 3C \rightarrow 3CO_2(g) + 4Al \quad (5)$$

- Aluminium reoxidation reaction, causing loss of current efficiency:

$$3CO_2(g) + 2Al \rightarrow Al_2O_3 + 3CO(g) \quad (6)$$

- Anode sulphur content is responsible for the appearance of SO_2 in the cell emissions. First COS is formed in the anode at higher temperatures. Subsequently, COS is burnt under the cell hood.

$$Al_2O_3 + 3C + 3S \rightarrow 2Al + 3COS(g) \quad (7)$$

$$2COS(g) + 3O_2(g) \rightarrow 2CO_2(g) + 2SO_2(g) \quad (8)$$

- Anode carbon air burn: Part of anode surface is exposed to air and it is hot enough to combust.

$$C + O_2(g) \rightarrow CO_2(g) \quad (9)$$

- Boudouard reaction: Part of carbon dioxide produced by electrolysis passes through the anode pores, an environment rich in carbon at high temperatures.

$$CO_2(g) + C \rightarrow 2CO(g) \tag{10}$$

- As an assumption, all the carbon monoxide produced by the reoxidation reaction and Boudouard reaction is burnt under the cell hood where the temperatures are usually around 150°C.

$$2CO(g) + O_2(g) \rightarrow 2CO_2(g) \tag{11}$$

- Hydrogen fluoride evolution from bath, alumina water content is responsible to provide hydrogen.

$$2AlF_3 + 3H_2O \rightarrow Al_2O_3 + 6HF(g) \tag{12}$$

- Sodium tetrafluoraluminate evolution from bath. The water involved here comes from air humidity.

$$Na_3AlF_6 + 2AlF_3 \rightarrow 3NaAlF_4(g) \tag{13}$$

$$3NaAlF_4(g) + 3H_2O(g) \rightarrow Al_2O_3 + Na_3AlF_6 + 6HF(g) \tag{14}$$

The determination of each individual species mass balance can be predicted by adopting reasonable assumptions. If duct gas flow composition measurements are available, all the analytical part of composition prediction is not compulsory, but it is recommended to be performed in order to check the consistency of modelling assumptions.

Cell Energy Balance

The cell heat balance obeys the 1st law of thermodynamics. The difference between heat inputs and outputs is the heat accumulation. The energy inputs are expressed by the enthalpy associated with the materials entering the cell plus the cell voltage heat production. The heat outputs are expressed by the enthalpy associated with the materials leaving the cell control volume plus the heat dissipation to ambient. The equation (16) presents the heat balance function of materials flow, Joule heat and dissipation to the ambient:

$$Q_{ac} = Q_{in} - Q_{out} \tag{15}$$

$$Q_{ac} = V_{Cell} I + \dot{w}_{Al} \left(\sum \dot{m}_{i\_in} H_i(T_{i\_in}) - \sum \dot{m}_{i\_out} H_i(T_{i\_out}) \right) - \frac{(T_B - T_A)}{R_{EqAp}} \tag{16}$$

Where Q is heat flow in [W], V_{cell} is cell voltage in [V], I is the line current in [A], $\dot{w}_{Al}$ is the aluminium production rate in [kg/s], $\dot{m}_i$ is the massflow rate per kg of aluminium of substance "i" [kg/kg Al], H_i is the enthalpy in [J/kg] at Temperature T_i, T_A is the ambient temperature in [°C], T_B is the bath temperature in [°C] and R_{EqAp} is the equivalent thermal resistance of the cell from the bath to the exterior in [°C/W]. Some authors [2, 11] prefer to express the cell energy balance as a cell voltage balance, dividing all equations by "*I*". However, such an approach should be carefully applied because the first law of

thermodynamics states the conservation of only mass and energy. Voltage equations are not valid for transient calculations or if the cell presents current path disturbances.

Energy Source: Cell Voltage and Line Current

In the smelters, the electrical energy input into the cell is very well monitored and controlled in real time by measuring the total voltage and line current. In the past, many efforts have been made [16, 17] to study in detail the parts of the total cell voltage. However, for the cell energy balance purposes presented in this paper, it is irrelevant to know the exact values of the "voltage breakdown" because all voltage parcels will end up in the form of energy generation inside the cell control volume.

Energy Sink Associated with Mass Balance

After the implementation of the mass balance, the enthalpy balance associated with all materials can be established. The enthalpy associated with a certain mass of a substance at temperature T is:

$$H_i(T) = \Delta_f H_{298}^0 + \int_{298}^{T} C_p(T)dT \tag{17}$$

The first part of the right hand side of equation is the enthalpy of formation for the substance. The specific heat $C_p(T)$ is usually represented by a polynomial function of temperature found in thermodynamic tables. The total heat sink of the cell is represented by sum of all substances enthalpy entering and leaving the cell control volume:

$$\Delta H_{Tot} = \left(\sum \dot{m}_{i\_in} H_i(T_{i\_in}) - \sum \dot{m}_{i\_out} H_i(T_{i\_out}) \right) \tag{18}$$

If good modern cell operation is considered, the heat sink calculated by equations above is expected to be in the order of ~ 8 - 9 [kWh/kg Al]. It includes the amount of energy transferred from the cell interior to the gases leaving the cell duct. It is possible to define the minimum heat sink for alumina reduction that is obtained calculating the enthalpy difference between products (Al, CO_2) at reaction temperature T_B and reactants (C, Al_2O_3) at ambient temperature T_A:

$$\Delta H_{Min} = \left(H_{Al}(T_B) + \frac{3M_{CO_2}}{4M_{Al}} H_{CO_2}(T_B) \right) - \left(\frac{M_{Al_2O_3}}{2M_{Al}} H_{Al_2O_3}(T_A) + \frac{3M_C}{4M_{Al}} H_C(T_A) \right) \tag{19}$$

Where "M_i" is the molar mass of substance "i". If we start from pure gamma alumina, the result for the ideal minimum required energy for aluminium production is 6.25 [kWh/kg Al] at T_A=25°C and T_B=960°C. The cell energy efficiency "E_{eff}" can be defined as the ratio between the minimum energy required for the reduction reaction and the total energy provided to the cell.

$$E_{Eff} = 100 \frac{\Delta H_{Min} \dot{w}_{Al}}{V_{Cell} I} \tag{20}$$

The best aluminium smelters in the world present energy efficiency in the order of 50%. Some older technologies produce at energy efficiencies as low as 40%.

Heat Losses to Environment: Analogue Thermal Resistances Model

If steady state condition is assumed (no accumulation Q_{ac}=0), the heat losses are usually described using the so called 2-zones approach [11, 18, 19]. It can be represented by 2 parallel series of thermal resistances, connecting the bath temperature (heat input location) to the environment temperature (heat output location).

We propose a 3-zone description, where the heat flowing through the cell top insulation leaves the cell at duct temperature and not at environment temperature. Figure 7 shows the analogue thermal circuit representing the cell heat losses of the 3-zones approach and Figure 8 shows a schematic representation of resistances inside the cell. There are three parallel groups of thermal resistances: one for the heat passing through the ledge and cell walls, one for the bottom heat flow without ledge and another for the top heat losses to the duct air collection.

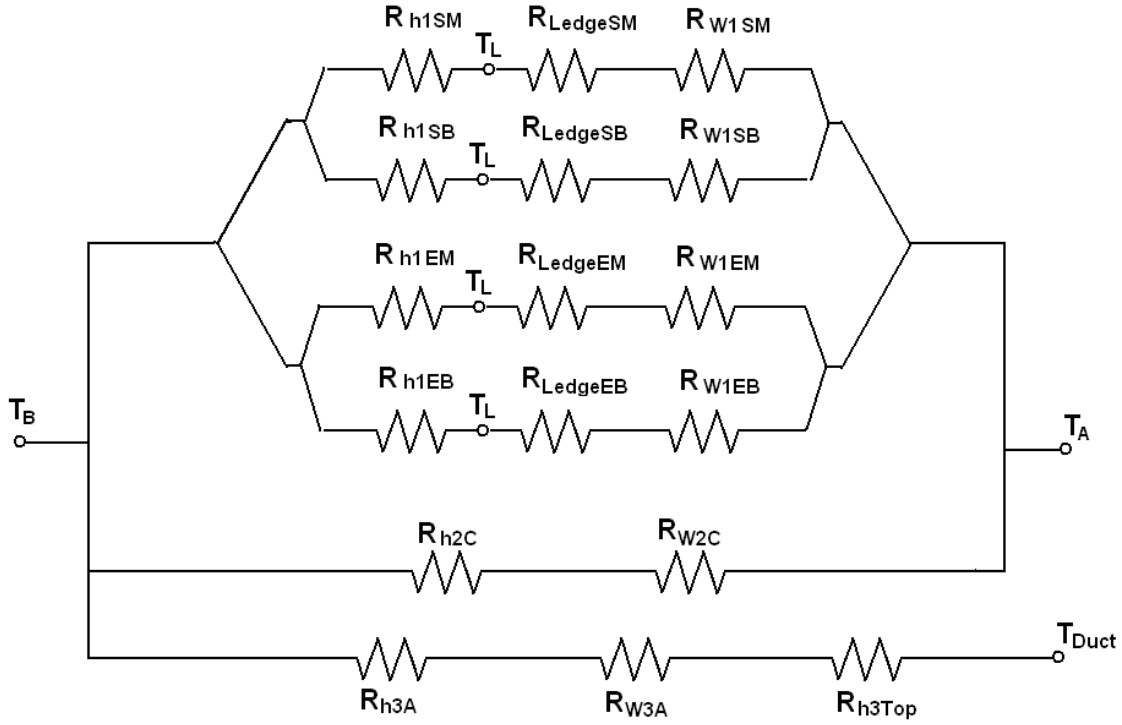

Figure 7: Thermal resistances representing cell heat losses

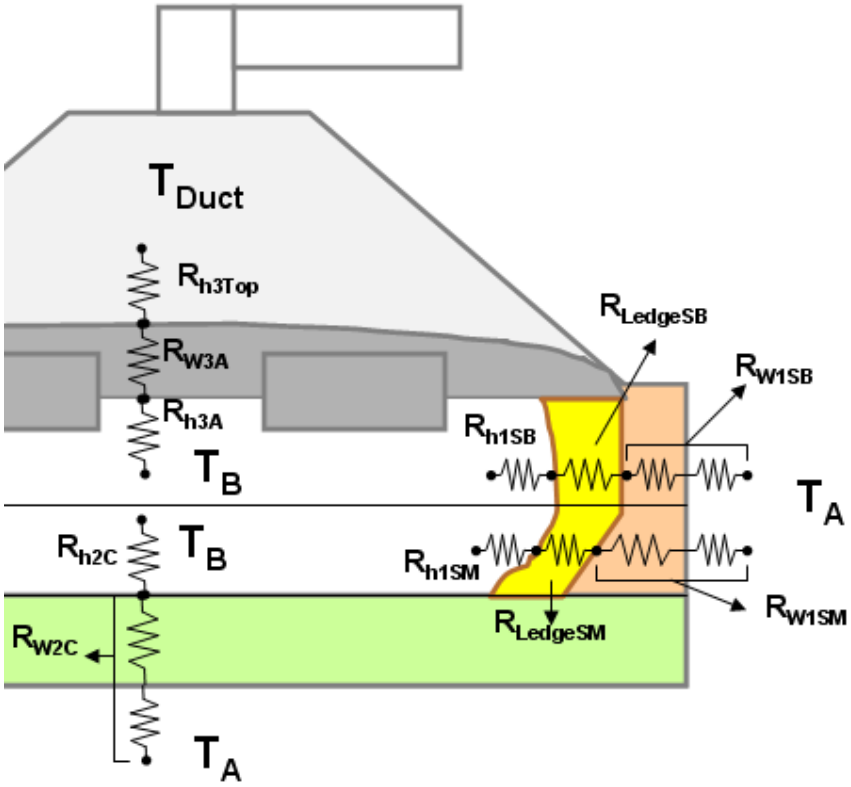

Figure 8: Schematic representation of thermal resistances inside the cell (sidewall cut view, for endwall cut view, subscript "W" is substituted by "E")

Nomenclature: "R" is thermal resistance, subscripts define the resistance position: "W" stands for wall, "M" is metal level, "B" is bath level, "h" is convective resistance at fluid-solid interfaces, "C" is cathode panel, "A" is anode panel, "S" is sidewall and "E" endwall. Note: for simplicity, we represented wall resistances "R_W" as the sum of solid conductive resistance and external natural convection resistance around the shell.

One series of resistances conducts a certain heat flow "Q_1" through the regions covered by frozen bath. In this region, the superheat plays the major role as "driving force", determining the heat flow and ledge thickness. The other two series of thermal resistances conducts the "Q_2" and "Q_3" heat through the regions not covered by frozen bath, generally, anode panel and the cathode blocks. The heat flow is proportional to delta temperature between liquid bath and environment (for cell bottom) and between liquid bath and duct temperature (for cell top). Thermal resistances at anode panel may not be constant, due to cover variation, or due to the "apparent" thermal resistance increase by heat generation inside the electrodes, pins, yoke, guide rods. Liquidus temperature is a function of bath chemistry and bath temperature is calculated iteratively considering heat generation and losses, cell voltage and ACD.

Cell Lining and Shell Thermal Resistances

In this approach, the thermal resistances are obtained by a 3D finite element model (Figure 9). If cell geometry or electrode properties or insulation properties are modified, then the 3D model has to be recalculated to obtain new resistance values. The shielding effect of heat generation inside the electrical conductors due to Joule effect is also obtained by the 3D auxiliary model.

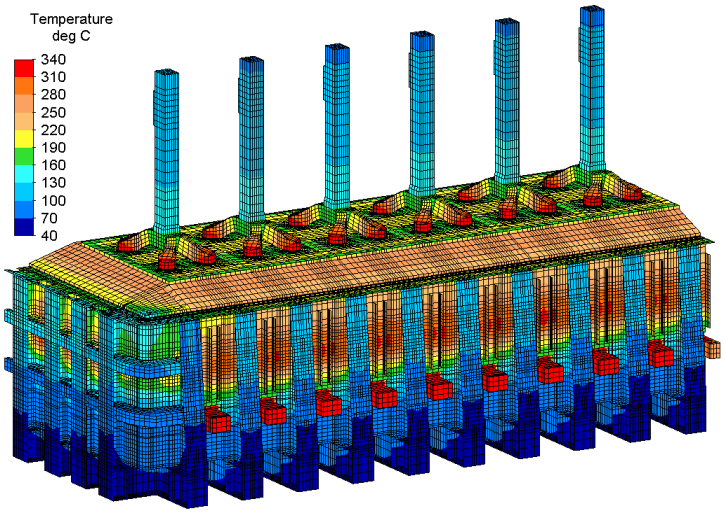

Figure 9: 3D electrolytic cell thermal electric submodel, external view of calculated temperatures.

Cell Top Heat Losses

The cell top heat transfer resistance is a combination of bath convective heat transfer coefficient, conduction through the anode carbon and cover/crust plus convection and radiation under the cell hood. In order to study the effect of duct flow rate on the top heat losses, another CFD model is applied. The boundary conditions and calculated gas temperature field are shown in Figure 10 and Figure 11, respectively. The output cell duct temperature is found by the model for a given duct flow rate, bath temperature and potroom temperature. In addition, hot gases evolved from bath are included in the sub model, and as well, the carbon airburn heat sources.

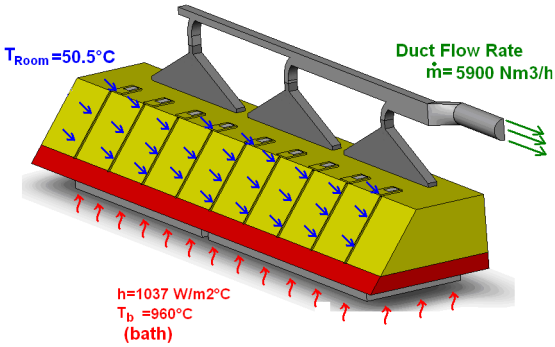

Figure 10: Boundary conditions of the gas collection submodel

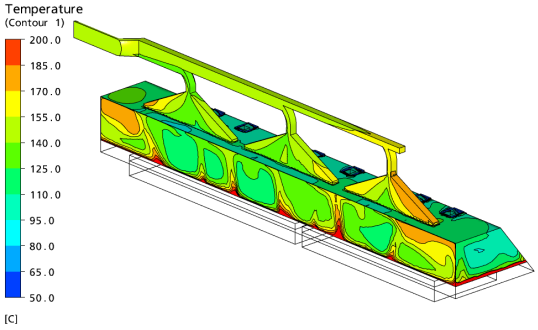

Figure 11: Temperature distribution of the cell gas calculated by the gas collection submodel

Changes in the duct flow rate have a limited effect on the energy flow of the cell top. Typically, estimations show that around one third of cell top thermal resistance is convective (gas-cover). The other two thirds are anode panel and crust/cover material. The exact shares of each thermal resistance depend on cell technology and cover practices.

Convective Internal Thermal Resistances

The heat transfer coefficients between bath and ledge and metal and ledge are key factors in the prediction of ledge size and heat flux through the cell walls. In the present work, these

coefficients are calculated using the same published models [7] developed at CAETE. The modelling results are in accordance with the magnitudes found in the compilation of experimental and analytical results published by Solheim [20], more details concerning the boundary conditions and results are found in an earlier paper [7].

Cell Mass and Energy Balance Model

The Figure 12 presents a flowchart of the complete heat and mass balance modelling. The 3D electromagnetic model provides MHD forces for fluid flow calculation at metal. In parallel, the gas induced flow is evaluated at the bath. Once the fluid flow is obtained, wall heat transfer coefficients at the ledge, anode and cathode surfaces as well as the top cover heat transfer coefficients are calculated. These coefficients are supplied to the thermal 3D sub-model and also to the global cell balance model. The 3D sub-models supply the balance model with the wall thermal resistances for a given cell design. Finally, the global cell balance model processes all the inputs and determines the resultant cell state: bath composition, mass balance for each substance, associated heat balance and ledge thickness prediction.

The global balance model is implemented in Visual Basic computational code named "Cell Mass & Energy Balance". The program solves mass and energy balances for a cell in averaged steady state condition. The user must provide a set of data regarding: raw materials (gross and net carbon consumption, alumina impurities), measured cell parameters (voltage, current, CE). The thermal resistances obtained by 3D models are inserted in the advanced user area.

When all inputs are properly defined, the user can easily calculate and modify operation parameters, such as: line current, bath composition, cathode resistance, bath temperature, metal and bath depth, alumina composition and other material input quantities for a new cell state recalculation. The Figure 13 shows an example of the input data filled screen in the Cell Mass & Energy Balance computational code.

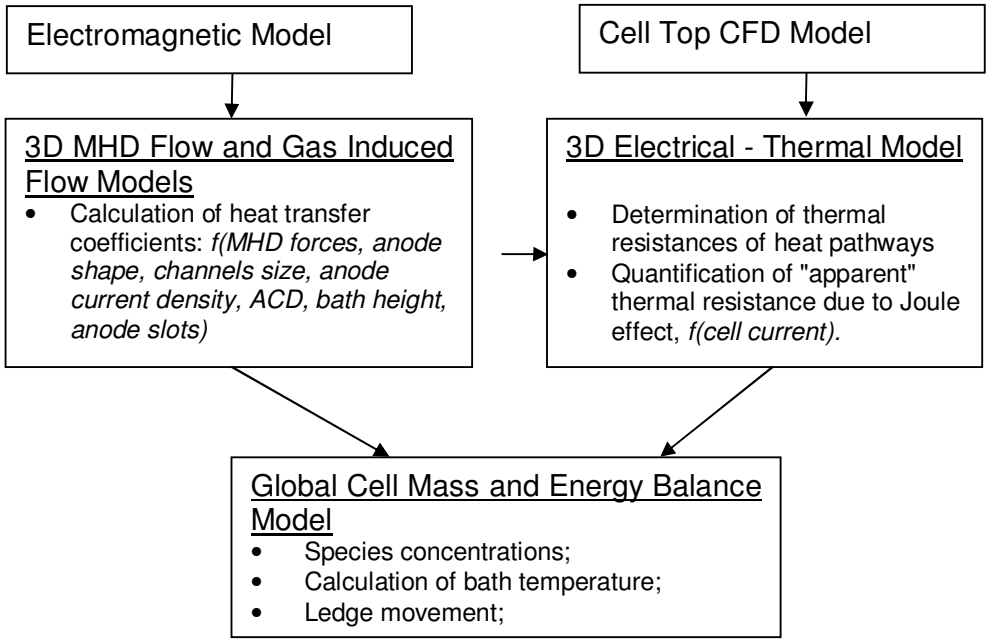

Figure 12: Models flowchart

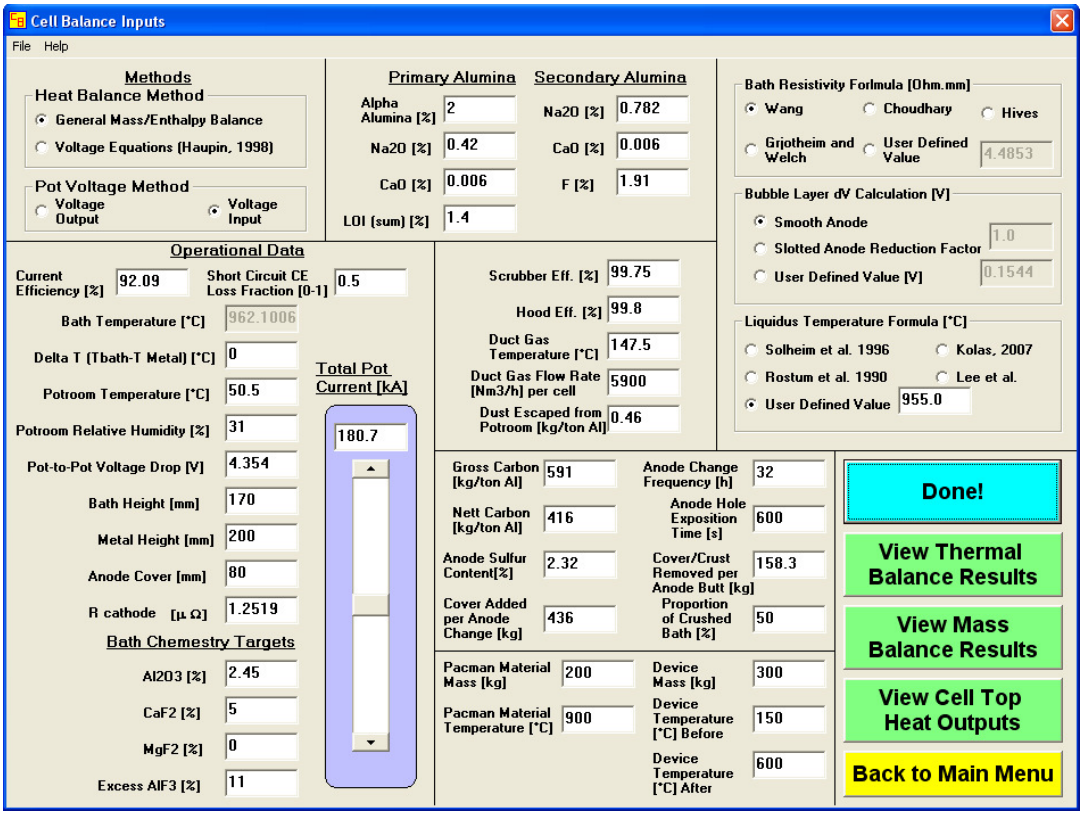

Figure 13: Input Data Screen of the "Cell Mass & Energy Balance V.1.01" program.

The next sections present results of mass and energy balance calculation using the Cell Mass & Energy Balance program.

Case Study: 180kA cell

Let us consider the cell data as shown in the Figure 13 and the additional information regarding the anode assembly:

- Mass of 1 Guide Rod (aluminium): 117 [kg];
- Mass of 1 Yoke +Cast Iron (iron): 317 [kg];
- Extracted anode butt average temperature: 870[°C];
- Cover (extracted with anode butt), average temperature:590 [°C];
- Guide Rod (extracted with anode butt), average temperature:135 [°C];
- Yoke +Cast Iron (iron) (extracted with anode butt), average temperature: 386 [°C];
- Cell thermal resistances were obtained by 3D Finite Element models (Figure 9), heat transfer coefficients at ledge were obtained by 3D CFD models and inserted and inserted in the Cell Mass & Energy Balance Code.

Mass Balance Results

The information above was inserted in the Cell Mass & Energy Balance code and the mass balance of each species was obtained. The Figure 14 shows the resulting mass flow rates screen of input and output materials.

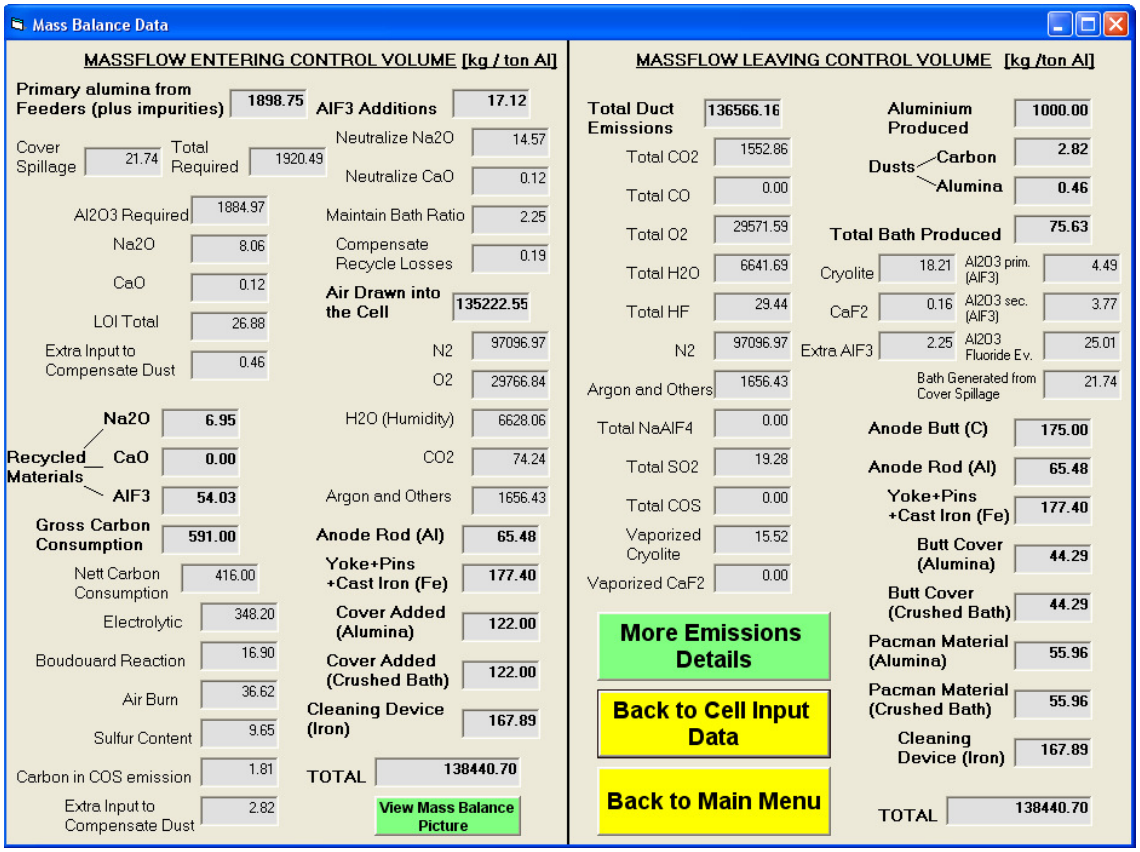

Figure 14: Cell mass balance results sheet obtained by the "Cell Mass & Energy Balance" code.

The total inputs and total outputs must be equal considering averaged steady state. One interesting application of the presented program is the determination of the cell duct gas chemical composition. Improvements on the process operation can be virtually tested. Examples: AlF_3 correction needs can be predicted. Actions to reduce emission rates can be studied. It is possible to assess the impact of changing alumina impurities composition on cell emissions. The role played by cathode cleaning material in the mass and energy balance can be quantified.

A special and more detailed screen of the Cell Mass & Energy Balance code was developed to show the contribution of many processes in each gaseous species generation or consumption, see Figure 15. Afterwards the remaining balance of each component leaves the cell by the collection duct.

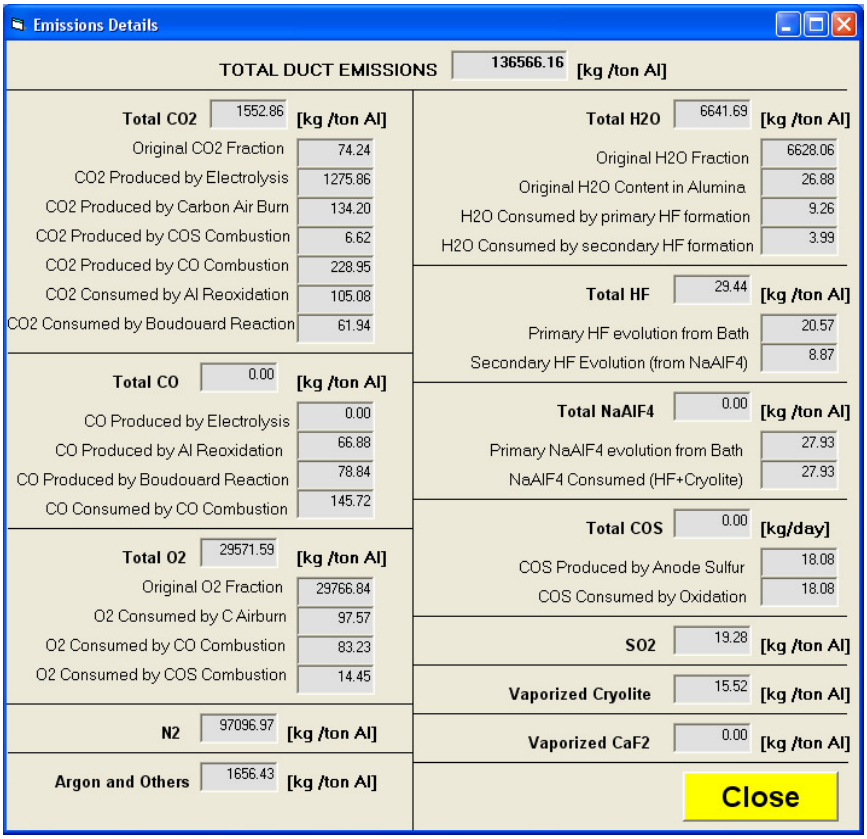

Figure 15: Detailed duct emissions result screen obtained by the "Cell Mass & Energy Balance" code.

Energy Balance Results:

The cell energy consumption can be divided in three types:

1. Thermodynamic unavoidable energy consumption in order to satisfy the alumina reduction reaction enthalpy (ΔH) and to heat the reactants (C, Al_2O_3) from the ambient temperature up to the reaction temperature (~960°C).

2. Energy consumption of parallel reactions (reactions involving fluorides, sulphur, Al reoxidation, etc.) and to heat up other materials not producing aluminium (alumina impurities, AlF_3, excess of carbon, anode butt materials, cathode cleaning materials, duct gases, etc.).

3. Energy dissipated by the cell walls in the convection + radiation processes, responsible to maintain the cell ledge and superheat at stable values.

The cell energy consumption breakdown is presented in Figure 16 using the mass balance method for the case above. It is impossible to reduce the energy consumption Type 1. The energy losses Type 3 are highly dependent on the cell thermal design and can be modified only by changing the ledge thickness (and superheat) or by changing the cell lining. The energy consumption Type 2 can be reduced by smelter operation with careful control of cell mass balance streams.

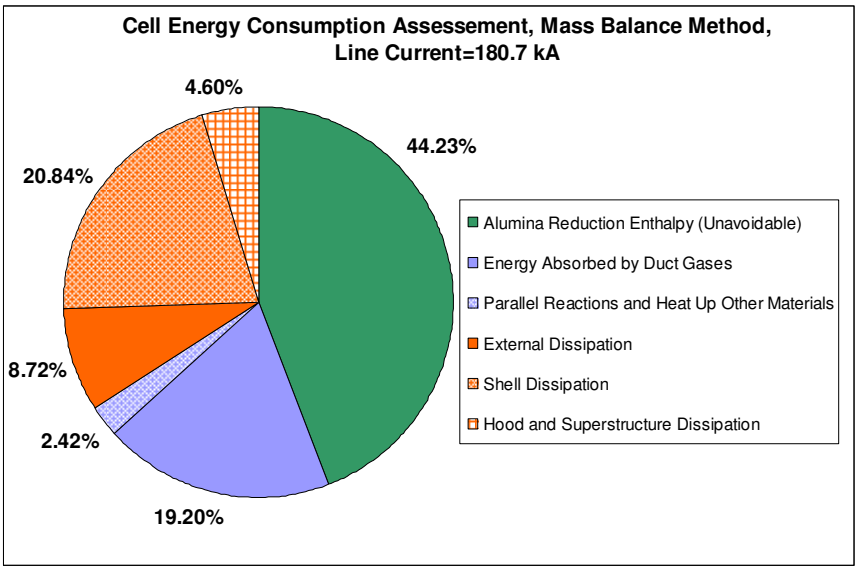

Figure 16: Cell energy consumption breakdown calculated by the mass balance method, Type 1: green, Type 2: blue, Type 3: orange.

The Table 1 shows the cell consumption results using the energy balance methodology proposed in this paper for 3 different cell currents compared with an example of "classic" approach [2]. Cell Voltage of 4.354 [V] was set for all cases, resulting in cell consumption of 14.090 [kWh/kg Al]. Energy consumption types are differentiated.

Table 1: Thermal balance results for different line currents using mass balance method. Last column presents a result using the classical method

	Mass and Energy Balance Method			Classic Method [2]
I [kA]	185.7	180.7	175.7	180.7
Cell Thermal Efficiency [%]	44.23	44.23	44.23	44.23
Total Cell Consumption [kWh/kg Al]	**14.090**	**14.090**	**14.090**	**14.090**
Enthalpy Balance (New Control Volume)	**9.171**	**9.277**	**9.390**	**NA**
Enthalpy Balance (Classic Control Volume)	6.571	6.573	6.575	6.377
Type 1: Alumina Reduction Enthalpy (Unavoidable)	**6.232**	**6.232**	**6.232**	**6.232**
Reaction Enthalpy at Bath Temperature	5.655	5.655	5.655	5.655
Al_2O_3, C Heat Up to the Reaction Temperature	0.577	0.577	0.577	0.577
Type 2: Heat up Materials and Parallel Reactions	**2.939**	**3.045**	**3.158**	**NA**
Energy Absorbed by Duct Gases	2.600	2.704	2.815	NA
Other Reactions and Heat Up	0.339	0.341	0.343	0.144
Type 3: Energy Dissipation to the Potroom	**4.919**	**4.813**	**4.701**	**5.009**
External Dissipation (Busbar)	1.262	1.228	1.194	1.228
Shell Dissipation	3.026	2.937	2.84	3.133
Hood and Superstructure Dissipation	0.631	0.648	0.667	0.648

The most important observed difference is that the classic methods often underestimate the energy spent in minor chemical reactions and to heat up many materials such as: alumina impurities, anode carbon and other parts, fluoride additions, cathode cleaning materials. In

the classic method [2], only the reoxidation reaction is taken into account besides the electrolysis reaction. This also overestimates the predicted cell losses to the potroom, leading to lower expected ledge thickness.

Energy Losses Associated with Cell Duct Flow Rate

The largest share of cell energy consumption Type 2 is carried by the duct gases, representing an important opportunity to save energy. It is worthy to study and optimize the cell duct flow rate and unfortunately sometimes it is ignored in many cell thermal models. In the studied case, the duct flow can be decreased from 5900 [Nm^3/h] to 4000 [Nm^3/h] and the new duct temperature is predicted by the CFD model to be 20.5°C higher (168°C). Assuming the same cell current (180.7 kA), ledge thickness and shell heat flow and that there is room for ACD squeeze, cell consumption can be reduced from 14.090 [kWh/kg Al] to 13.401 [kWh/kg Al] only by modifying the duct flow rate, see The Table 2 results comparison for both flow rates.

Table 2: Thermal balance results using mass balance method, for different cell duct flow rates.

	Duct Flow: 5900 Nm^3/h	**Duct Flow: 4000 Nm^3/h**
Total Cell Voltage [V]	**4.354**	**4.141**
Total Cell Consumption [kWh/kg Al]	**14.090 (100%)**	**13.401 (100%)**
Type 1: Alumina Reduction Enthalpy (Unavoidable)	**6.232 (44.23%)**	**6.232 (46.50%)**
Reaction Enthalpy at Bath Temperature	5.655 (40.13%)	5.655 (42.20%)
Al_2O_3, C Heat Up to the Reaction Temperature	0.577 (4.10%)	0.577 (4.31%)
Type 2: Heat up Materials and Parallel Reactions	**3.045 (21.61%)**	**2.356 (17.58%)**
Energy Absorbed by Duct Gases	2.704 (19.19%)	2.015 (15.04%)
Other Reactions and Heat Up	0.341 (2.42%)	0.341 (2.54%)
Type 3: Energy Dissipation to the Potroom	**4.813 (34.16%)**	**4.813 (35.92%)**
External Dissipation (Busbar)	1.228 (8.72%)	1.228 (9.16%)
Shell Dissipation	2.937 (20.84%)	2.937 (21.92%)
Hood and Superstructure Dissipation	0.648 (4.60%)	0.648 (4.84%)

Note that the cell energy efficiency increased to 46.5% and the new cell voltage was reduced to 4.141V. In fact, the gas duct flow can be used to regulate cell heat dissipation breakdown in a limited extent. The same effect can be obtained by modifying the cover thickness.

Other Cell Material Flow Energy Losses

Around 0.35 [kWh/ kg Al] (2%-3%) of cell energy is consumed by parallel materials heat up and reactions (excluding air heat up) inside the cell. This fraction is important for precise cell energy balance calculations. Energy is lost by several processes worthy of investigation: excess of carbon consumption, stored anode butt energy including hot cover, yoke and guide rod, radiation from open cavity exposition, cavity cleaning material losses, alumina impurities heat up, aluminium fluoride heat up and reaction.

All these contribution can be evaluated with the heat and mass balance calculations. The Figure 17 shows the resulting energy losses associated with each one of these processes for the studied cell technology.

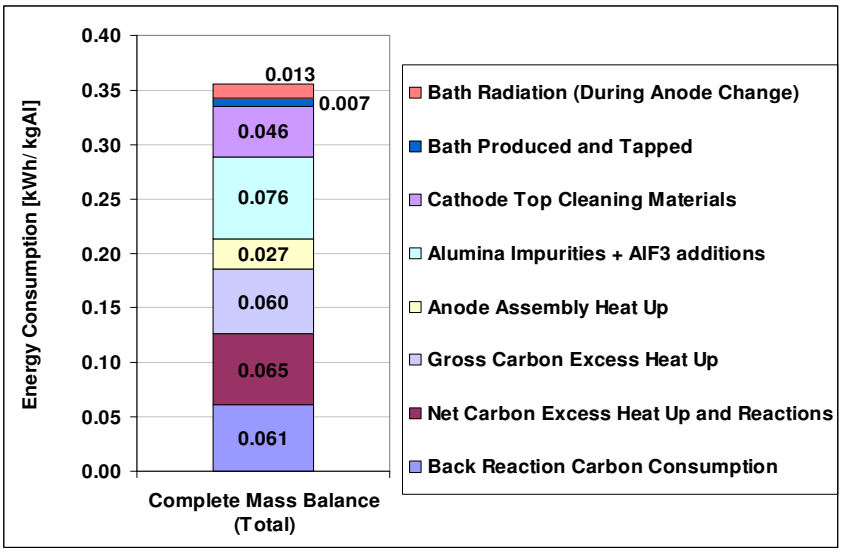

Figure 17: Energy consumption associated with the minor cell material flow and parallel reactions

Actions to minimize these energy losses are possible, for example: reduce time spent per anode change, improve the cover practices to generate less sludge, reduce gross and net carbon consumptions, etc.

Energy Losses Associated with Cover Practices

In the studied case, 436 kg of cover material is added to the cell at each anode change. The cover leaves the cell control volume in a variety of forms: part remains on the anode butt top leaving the cell at anode change, part falls over the cathode and leaves the cell during cathode cleaning, part dissolves into the bath 50% alumina is consumed and the other 50% forms more bath and, occasionally, it is tapped out. Assuming that the cathode cleaning material composition (200 kg) is the same as original cover, the share of each destination of the cover material is shown in Figure 18.

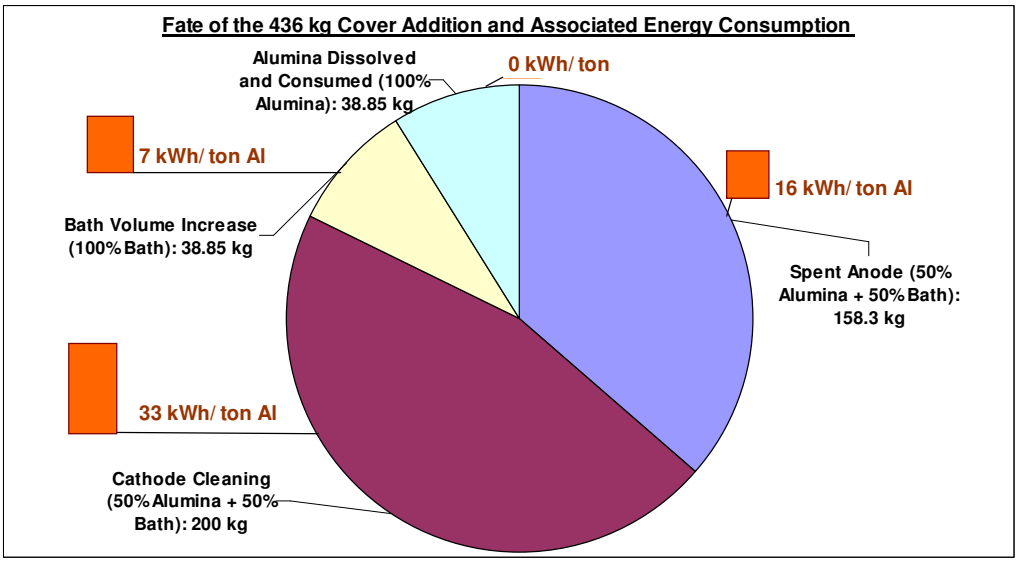

Figure 18: Estimation of cover material fate in studied case and the energy lost with material flow in each material flow (orange bars and values)

The energy loss associated with cathode cleaning material is the most relevant because it comes out of the cell at almost the bath temperature (~960°C), while the anode butt cover is at ~600°C. Eventually, bath production must be tapped out also at bath temperature. The alumina content of cover dissolved into the bath contributes to make aluminium and thus, by definition, no cell energy inefficiency comes from this process.

Conclusions

In general, traditional cell energy balance models underestimate the heat losses due to material balance because the contributions of many materials are ignored. This fact can lead to wrong cell operating window and ledge thickness predictions. Another advantage of a detailed material balance calculation is the possibility to study cell emission rates and AlF_3 needs in the entire context of the cell heat and mass flow balance, evaluating all influences and consequences simultaneously.

The cell heat lost to the duct gases represents a very important share of the cell energy consumption. Using the modelling methodology presented in this paper, the prediction of the duct flow rate versus heat balance impact was made. A lower duct flow rate reduces heat losses opening the possibility for energy saving, but reduces the cell emissions capture efficiency. A compromise solution has to be found for the optimal cell duct flow. In some cases, when cell current is increased and more heat has to be extracted from the cell, the increase of cell duct flow rate can be applied to re-equilibrate the heat losses and ledge thickness of the cell.

The cell energy balance is influenced by operational practices, and this fact has to be explored when fine tunning electrolytic cell efficiency. The anode change duration and dressing cover addition affect the cell heat losses and should be minimized, as well the carbon excesses. Cathode surface or cavity cleaning can be responsible for 0.05-0.1 [kWh/kg Al] of energy losses. Lower cover consumption reduces the cell heat losses. Alumina impurities are responsible for another 0.05-0.1 [kWh/kg Al] additional energy consumption.

References

1. B. J. Welch, J. T. Keniry: Advancing the Hall-Heroult Electrolytic Process, *TMS Light Metals* 2000, pp 17-26.
2. W. E. Haupin, Interpreting the Components of Cell Voltage, *TMS Light Metals* 1998, pp 531-537.
3. M. Dupuis: Computation of Aluminum Reduction Cell Energy Balance using ANSYS ® Finite Element Models, *TMS Light Metals* 1998, pp 409-417.
4. P. Biedler: Modeling of an Aluminum Reduction Cell for the Development of a State Estimator, *College of Engineering and Mineral Resources at West Virginia University PHD Thesis*, Morgantown, West Virginia, USA, 2003.
5. T. R. Beck: The Relation of Gas Composition to Current Efficiency in an Aluminum Reduction Cell, *Journal of Electrochemical Society, Volume 106*, pp 710-713.
6. Cooksey M. A., Yang W., "PIV Measurements on Physical Models of Aluminium Reduction Cells", *TMS Light Metals* 2006, pp 359-365.
7. D. S. Severo, V. Gusberti: A Modelling Approach to Estimate Bath and Metal Heat Transfer Coefficients, TMS Light Metals 2009, pp 557-562.

8. L. Tikasz, R. T. Bui, V. Potocnik: Aluminium Electrolytic Cells: A Computer Simulator for Training and Supervision, *Engineering with Computers (1994) 10*:12-21, Springer-Verlag London Limited, 1994.
9. I.Tabsh, M. Dupuis, A. Gomes: Process Simulation of Aluminum Reduction Cells, *TMS Light Metals* 1996, pp 451-457.
10. T. Drengstig: On Process Model Representation and AlF_3 Dynamics of Aluminum Electrolysis Cells" *Dr. Ing. Thesis, Department of Engineering Cybernetics - Norwegian University of Science and Technology*, Trondheim-Norway, August 1997.
11. J. N. Bruggeman: Pot Heat Balance Fundamentals, *6th Australasian Aluminum Smelting Workshop Proceedings,* Queenstown, New Zealand, 22-27th November 1998, pp 167-189.
12. O. O. Rodnov, P.V. Poliakov, A. I. Berezin, P. D. Stont, I. V. Mezhubovsky: Estimation of a Technological Condition of the Aluminium Reduction Cells on the Basis of its Daily Energy Balance, *TMS Light Metals* 2003, pp 457-462.
13. T. V. Piskazhova and V. C. Mann: The Use of a Dynamic Aluminum Cell Model, *JOM—Journal of the Minerals, Metals and Materials Society, 58*(2), 2006, pp 58-62.
14. S. Kolas, T. Stoere: Bath Temperature and AlF_3 Control of an Aluminium Electrolysis Cell", *Control Engineering Practice 17* (2009), pp 1035–1043.
15. M. Iffert: Aluminium Smelting Cell Control and Optimization. *Chemical Sciences & Engineering, Faculty of Engineering, UNSW. PhD Thesis*, 2007.
16. J. Thonstad, E. Hove: On the Anodic Overvoltage in Aluminum Electrolysis, *Canadian Journal of Chemistry, Volume 42*, 1964. Pp 1542-1550.
17. J. Thonstad, S. Rolseth: On the Cathodic Overvoltage on Aluminium in Cryolite-Alumina Melts-I, *Electrochemica Acta, Volume 23*, 1978, pp 223-231.
18. F. Stevens: Reduction Cell Energy Balance Dynamics and Performance, *5th Australasian Aluminium Smelting Technology Workshop Proceedings*, Sydney, Australia, 22-27th October 1995, pp 171-191.
19. L. I. Kiss, V. Dassylva-Raymond: Freeze Thickness in the Aluminum Electrolysis Cells, *TMS Light Metals* 2008, pp 431-436.
20. A. Solheim: Some Aspects of Heat Transfer between Bath and Sideledge in Aluminium Reduction Cells, *TMS Light Metals* 2011, 381-386.